Transcriptomic study of the toxic mechanism triggered by beauvericin in Jurkat cells

Toxicology Letters 284 (2018) 213–221

Contents lists available at ScienceDirect

Toxicology Letters

journal homepage: www.elsevier.com/locate/toxlet

Transcriptomic study of the toxic mechanism triggered by beauvericin in Jurkat cells

L. Escrivá[a,*], D. Jennen[b], F. Caiment[b], L. Manyes[a]

[a] Laboratory of Food Chemistry and Toxicology, Faculty of Pharmacy, University of Valencia, Burjassot, Spain
[b] Department of Toxicogenomics, GROW School for Oncology and Developmental Biology, Maastricht University, The Netherlands

ARTICLE INFO

Keywords:
Beauvericin
Jurkat
Immunotoxicology
RNA-seq
Toxicogenomics
Transcriptomics

ABSTRACT

Beauvericin (BEA), an ionophoric cyclic hexadepsipeptide mycotoxin, is able to increase oxidative stress by altering membrane ion permeability and uncoupling oxidative phosphorylation. A toxicogenomic study was performed to investigate gene expression changes triggered by BEA exposure (1.5, 3 and 5 μM; 24 h) in Jurkat cells through RNA-sequencing and differential gene expression analysis. Perturbed gene expression was observed in a concentration dependent manner, with 43 differentially expressed genes (DEGs) overlapped in the three studied concentrations. Gene ontology (GO) analysis showed several biological processes related to electron transport chain, oxidative phosphorylation, and cellular respiration significantly altered. Molecular functions linked to mitochondrial respiratory chain and oxidoreductase activity were over-represented (q-value < 0.01). Pathway analysis revealed oxidative phosphorylation and electron transport chain as the most significantly altered pathways in all studied doses (z-score > 1.96; adj *p*-value < 0.05). 77 genes involved in the respiratory chain were significantly down-regulated at least at one dose. Moreover, 21 genes related to apoptosis and programmed cell death, and 12 genes related to caspase activity were significantly altered, mainly affecting initiator caspases 8, 9 and 10. The results demonstrated BEA-induced mitochondrial damage affecting the respiratory chain, and pointing to apoptosis through the caspase cascade in human lymphoblastic T cells.

1. Introduction

Mycotoxins are secondary metabolites produced by filamentous fungi species with low-molecular weight and high variety of structural compounds. They represent one of the most important categories of biologically produced natural toxins relative to human health and economic impact worldwide, being found in numerous commodities of plant origin, especially cereals grains (Ruiz et al., 2011). Mycotoxins are practically unavoidable contaminants in food and feed representing among the natural food contaminants a major issue in food safety, and actually posing critical challenges in food toxicology (Dellafiora and Dall'Asta, 2017). Mycotoxin ingestion may induce various chronic and acute effects on humans and animals, such as cytotoxic, hepatotoxic, neurotoxic, genotoxic, immunosuppressive, estrogenic, nephrotoxic, mutagenic, teratogenic, and/or carcinogenic effects (Smith et al., 2016). Biochemically, the modes of action of mycotoxins can be divided into four categories: interactions with deoxyribonucleic acid (DNA), inhibition of different steps in protein synthesis, effects on cell membranes, and interfering on energy metabolism (Celik et al., 2010). From a molecular perspective, the primal mechanisms of toxic action commonly affect the integrity, functionality, and turn over of biological macromolecules −such as DNA, RNA, and proteins- or the biochemistry of the multitude of low-molecular-weight molecules (e.g. the production of reactive chemicals in cells) (Dellafiora and Dall'Asta, 2017).

Among the thousands of fungal secondary metabolites currently known, only a few groups of mycotoxins are important from the safety and economic points of view; namely aflatoxins, ochratoxin A, zearalenone, fumonisins and trichothecenes. However, several *Fusarium* species can produce a group of lesser-studied toxins called emerging mycotoxins, which includes beauvericin (BEA), enniatins, moniliformin, and fusaproliferin (Escrivá et al., 2015).

BEA is a cyclic hexadepsipeptide mycotoxin, which contains three D-hidroxyisovaleryl and three N-methylphenylalanil residues in an alternating sequence (Mallebrera et al., 2014). It shows insecticidal and antiviral properties, strong antibacterial activity against human, animal and plant pathogenic bacteria, and immunosuppressive effects (Wang and Xu, 2012). BEA, as lipophilic and ionophoric compound, was reported to increase ion permeability in biological membranes by forming a complex with essential cations (Ca^{2+}, Na^{+}, K^{+}) and cation-selective

* Corresponding author.
E-mail address: laura.escriva@uv.es (L. Escrivá).

https://doi.org/10.1016/j.toxlet.2017.11.035
Received 20 September 2017; Received in revised form 10 November 2017; Accepted 27 November 2017
Available online 01 December 2017

channels in lipid membranes, affecting the ionic homeostasis and uncoupling the oxidative phosphorylation (Tonshin et al., 2010). Consequently, BEA particulary disturbs the ion balance and the cytoplasmic pH in the mitochondrial membrane by the accumulation of Ca^{2+}, leading to increased levels of intracellular reactive oxygen species (ROS) and reduced intracellular glutathione (GSH) as signs of oxidative stress. The loss of mitochondrial membrane integrity may finally be conducive to degeneration and cellular necrosis and/or apoptosis (Schoevers et al., 2016).

The molecular cytotoxic mechanisms of many mycotoxins in animals still remain unclear and require further investigation, especially the depiction of the intact pathway and the alterations of key enzymes in the pathway driven by mycotoxins. The mitochondrial alterations and the relationship between oxidative stress and mitochondrial physiology induced by mycotoxins offer important research potential for elucidating the key steps of mycotoxicosis initiation (Wen et al., 2016).

Toxicogenomics aims to elucidate the molecular mechanisms of toxicity and modes of action by analyzing chemical induced changes in gene expression patterns (Li et al., 2016). Toxicogenomic approach could be used to understand the complex effects of chemicals and to assist in health risk assessment, and it has already generated interesting results for predicting compound genotoxicity and carcinogenicity (Wilson et al., 2013). Next generation sequencing (NGS) techniques will certainly become the gold standard for understanding molecular mechanisms of toxicity and they are revolutionizing genomic/proteomic studies providing high-throughput datasets with unprecedented precision and accuracy (Fang et al., 2012; Caiment et al., 2015). RNA-seq allows profiling gene expression and composition, and provides a combination of transcriptome-wide coverage, sensitivity, and accuracy for a comprehensive view of gene expression changes, contributing to a more detailed look at the transcriptome than the microarrays (Conesa et al., 2016).

A transcriptome analysis experiment was designed to characterize all transcriptional activity (coding and non-coding) in human Jurkat lymphoblastic T cells. The Jurkat cell line was selected as *in vitro* model system since it has frequently been used successfully in traditional *in vitro* studies of the immune system maybe because of its well established reliability (Shao et al., 2014). On the other hand, previous *in vivo* studies demonstrated that the emerging mycotoxins may reach bloodstream in detectable concentrations, allowing them to enter into direct contact with cells and other blood components (Manyes et al., 2014). The responses of Jurkat cells to immunotoxic mycotoxin deoxynivalenol were comparable with the responses of human peripheral blood mononuclear cells (Katika et al., 2012). Moreover, the Jurkat cell line makes experiments less labor-intensive and more reproducible as compared to primary cells, and they are of human origin facilitating extrapolation to the human situation.

The aim of this study was to investigate the changes in gene expression profile triggered by BEA in human Jurkat lymphoblastic T cells after 24 h of exposure (1.5, 3 and 5 μM).

2. Materials and methods

2.1. Reagents

The reagent grade chemicals and cell culture components used, RPMI-glutamax medium, penicillin/streptomycin, phosphate buffer saline (PBS), and BEA (783.95 g/mol, 97% purity) were purchased by Sigma chemical Co. (St. Louis, MO, USA). Dimethyl sulfoxide (DMSO) and methanol were obtained from Fisher Scientific (Madrid, Spain). Deionised water (resistivity < 18 MV cm) was obtained using a Milli-Q water purification system (Millipore, Bedford, MA, USA). Stock solution of BEA was prepared in methanol and maintained at −20 °C. Final concentrations of BEA in the assay were achieved by their dilution in the culture medium. The final methanol concentration in the medium was 1% (v/v).

2.2. Cell culture and beauvericin exposure

Jurkat cells (ATCC TIB-152) derived from human T lymphocyte peripheral blood were maintained in RPMI-glutamax medium supplemented with 100 U/mL penicillin, 100 mg/mL streptomycin and 10% (v/v) FBS inactivated. Incubation conditions were pH 7.4, 37 °C under 5% CO_2 and 95% air atmosphere at constant humidity. Culture medium was changed every two days. Absence of mycoplasma was checked routinely using the Mycoplasma Stain Kit (Sigma Aldrich, St Louis Mo. USA). Before contamination, cells were plated in 12-well tissue culture plates at a density of 5×10^5 cells/well. Jurkat cells were exposed for 24 h in standard conditions to 1.5 μM, 3 μM, and 5 μM BEA in 1% methanol and this solvent concentration as control (each condition n = 3) in maintenance medium.

2.3. RNA extraction and next generation sequencing (NGS)

Total RNA of the control and exposed human T lymphocytes cells was isolated using Direct-zol™ RNA MicroPrep kit and treated with RNase free DNaseI (Zymo Research) to remove genomic DNA contamination. The extracted RNA of each sample was firstly checked for quantity and quality using Agilent 2100 Bioanalyzer (Agilent Technologies). All sequenced samples were generated from high quality RNA samples having a RIN number above 8. The standard Illumina protocol was followed to develop RNA-seq libraries. The Illumina NextSeq 500 platform was used for sequencing. Then, one archive for each sample was obtained, 12 in total. RNA quality control and sequencing were carried out by the Genomics section of the Central Service for Experimental Research (SCIE, University of València).

2.4. Data processing

The latest versions of different analytical tools were used in order to achieve a RNA-seq differential gene expression analysis. Raw sequencing reads were pre-processed and quality control was first performed by FastQC software. Sequencing reads were aligned by Bowtie2 (v2.2.6) and mapped to the Ensembl Human genome sequence (GRCh38) using default parameters. Read counts of each gene were quantifyed using RSEM (v.1.2.28) and Normalization fitting a negative binomial distruction and pair comparison analysis (treated vs. control) were performed and DEGs were obtained using DESeq2 package. All the analyses were performed in R.

2.5. Gene expression analysis

All of the DEGs were subjected to over-representation and gene ontology (GO) analysis by ConsensusPathDB. GO annotations and functional classifications of DEGs were obtained. Pathway assignments were carried out using PathVisio software with *Hs_Derby_Ensembl_85 bridge* gene dataset. Adjusted $p \leq 0.05$ and z-score > 1.96 were used as the threshold to identify the significantly enriched GO terms and pathways.

2.6. Primer design and quantitative real-Time PCR assays

Gene-specific primers were designed using Primer-BLAST (http://www.ncbi.nlm.nih.gov/tools/primer-blast/) using default criterion of the software with amplified products ranging from 75 to 150 bp and Tm at 59 °C. Primer sequences used in the qRT-PCR analyses are presented in Table 1.

Standard RT-PCR was performed for all the primer pairs and a single amplification product of the expected size for each gene was obtained by the melting curve assay. Primer amplification efficiency was determined from standard curve generated by serial dilution of cDNA (5 fold each) for each gene in triplicate. Correlation coefficients (R^2 values) and amplification efficiencies (E) for each primer pairs were

Table 1
Primers Used for Real-Time Quantitative RT-PCR Analysis.

Gene Symbol	Primer sequences (5′ to 3′) FP/RP	E (%)	Regression coefficient (R^2)
MATN4	TGCAGGGCCATTGACTACTG/ TCGCTCACACACTGGAACTC	117	0,966
MT-ND3	GACTACCACAACTCAACGGC/ GGGCTCATGGTAGGGGTAAA	82	0,991
18S rRNA	CGGCTACCACATCCAAGGAA/ GCTGGAATTACCGCGGCT	76	0,994

calculated from slope of regression line by plotting mean Cq values against the log cDNA dilution factor in Stepone software. Real-time amplification reactions were performed in 96 well plates using SYBR Green detection chemistry and run in triplicate on 96-wells plates with the StepOne Plus Real-time PCR machine (Applied Biosystems). Reactions were prepared in a total volume of 10 µl containing: 3 µl of 1:2 diluted template, 1 µl of each amplification primer (5 µM) and 5 µl of 2× Fast SYBR Green (Applied Biosystems). Non-template controls (NTC) were also included for each primer pair, replacing the template by water DNAse and RNAse free from the RNA extraction kit (Zymo Research). The cycling conditions were set as default: initial denaturation step of 95 °C for 5 min to activate the Taq DNA polymerase, followed by 40 cycles of denaturation at 95 °C for 15 s, annealing at 59 °C for 30s. The melting curve was generated by heating the amplicon from 60 to 90 °C. Baseline, threshold cycles (Ct) and statistical analysis were automatically determined using the StepOne Plus Software version 2.3 (Applied Biosystems). All the experiments were done according to MIQE (Minimum Information for Publication of Quantitative Real-Time PCR Experiments) guidelines (Bustin et al., 2009).

3. Results and discussion

3.1. RNA extraction, sequencing and quantification

The highly abundant ribosomal RNA (rRNA) constitutes over 90% of total RNA in the cell and should be removed by an appropriate RNA-extraction protocol to acquire the messenger RNA (mRNA) (Conesa et al., 2016). RNA-seq data acquisition, which consists of several steps from obtaining raw reads to read alignment and quantification, was specifically checked at each step to monitor the quality of the data. Percentage of mapped reads, considered an important mapping quality parameter, was 43458513 indicating high overall sequencing accuracy and low presence of contaminating DNA and it was calculated by FastQC, version 0.11.3 (Andrews, 2010). The RNA Integrity Number (RIN) was above 8 and rRNA ratio (28S/18S) was above > 1.7, both obtained by the Eukaryote Total RNA Nano assay (Bioanalyzer, Applied biosystems).

3.2. Gene expression profile

The overall gene expression of lymphocytes T treated cells with three BEA doses (1.5, 3 and 5 µM) for 24 h significantly differed from the expression of untreated cells. Perturbed gene expression was shown in all studied concentrations when compared with control samples, with an increased number of differential expressed genes (DEGs) with increased dose, pointing to a concentration dependent damage. The number of DEGs in comparison of control samples raised from 44 to 2403 and 5511 when BEA exposure doses to Jurkat cells increased from 1.5 to 3 and 5 µM, respectively. The total number of identified DEGs considering all three BEA concentrations was 5719, with 60.4% down-regulation and 39.6% up-regulation (3457 and 2262 genes, respectively). This indicated a slight trend towards down-regulation against up-regulation after BEA exposure to Jurkat cells, also evidenced when analyzing each independent dose. In this way, the down-regulated genes ranged 61–80% of the total DEGs for each individual concentration, while the up-regulated ones represented between 21 and 44%.

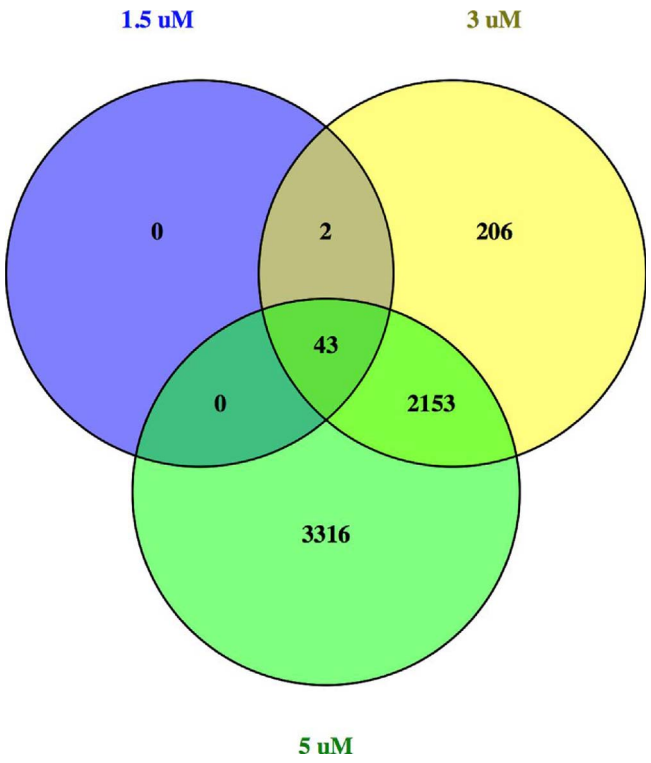

Fig. 1. Venn diagram for the differentially expressed genes in Jurkat cells treated with BEA at 1.5, 3 and 5 µM.

On the other hand, considering that the total human genome contains ~21000 protein coding genes (HGNC database), the results showed that BEA may compromised the normal expression levels up to 27.3% of human genome perturbation (16.5% down-regulation and 10.8% up-regulation). As it was expected, the highest dose (5 µM) compromised most the gene expression profile of the human genome, with similar values that those obtained in the general overview (10% and 16% up- and down- regulation, respectively). Among these 5719 DEGs identified for at least one BEA dose, 62% (3523 genes) were significantly perturbed in one single dose, mainly 5 µM (58%) and in lesser extent 3 µM (4%), with no one identified in lowest concentration (1.5 µM). On the other hand, around 38% (2154 genes) overlapped in two doses, almost all (99.9%) in the highest ones, 3 and 5 µM, indicating evidence of dose-dependent expression. Finally, 43 differentially expressed genes were found for each of the three studied BEA concentrations, considering them the most relevant geneset (Fig. 1).

3.3. Differentially expressed genes (DEGs)

Generating an accurate list of differentially expressed genes is the basis for pathway or gene set enrichment analysis (Fang et al., 2012). From the 43 DEGs found in the present study overlapping in the three studied BEA concentrations, 36 were down-regulated and 7 up-regulated. Moreover, 11 genes were located in the mitochondrial DNA, representing the 26% of the geneset. Interestingly, these 11 mitochondial DNA genes corresponded to the 10 most strongly down-regulated genes plus the most strongly up-regulated one, reaching Log2 fold change (Log2FC) values up to 3.6 in over-expression and −1.30 for repression. These results bring greater relevance to mitochondria as a target site for BEA induced cytotoxicity in cellular models. Moreover, the Log2FC values show a dose dependent expression pattern for all three BEA concentrations (Fig. 2).

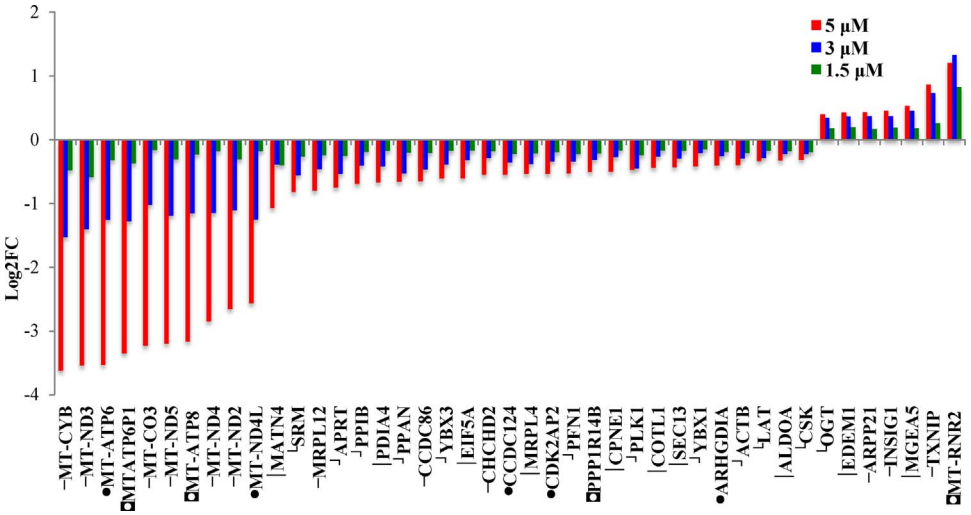

Fig. 2. Log2FC values for the differentially expressed genes overlapped in the three BEA concentrations; 1.5, 3 and 5 µM.

Mitochondria are the center of cellular energy homeostasis and redox regulation, and integrate numerous metabolic pathways, which may play a crucial role of initiative apoptosis. Though the majority (98%) of mitochondrial proteins is nuclear-encoded, the mitochondrial genome retains some genes encoding proteins involved in the respiratory chain. The mitochondrial respiratory chain complex gene family includes genes found in both nuclear DNA as well as mitochondrial DNA, and mutations in either nuclear or mitochondrial genes may cause diseases (Qi et al., 2017). In terms of apoptosis signaling, the mitochondria are a central sensor and integration point for diverse apoptosis signals (Lee et al., 2008). Mitochondrial integrity is central to both caspase-dependent and −independent cell death pathway, since its membrane perforation serves to induce both. The release of pro-apoptotic factors from the mitochondrial intermembrane space is a key event in a cell's commitment to die and is under the tight regulation of the Bcl-2 family. However, the underlying mechanisms governing the efflux of these pro-death molecules are largely unknown (Donovan and Cotter, 2004). BEA-treated cells have the ability to complete the entire apoptotic process and result in cell fragmentation (Jow et al., 2004). The results obtained in the present study increase the scientific evidence through the transcriptomic approach that mitochondria are the main cell organelle responsible of BEA induced toxicity.

The rest of the 43 DEGs were distributed into different chromosomes highlighting chromosomes 16 (12%), 17 and 7 (9% each), followed by 1, 3, 11 and 19 (7% each). Table 2 shows the geneset list including the HGNC symbol, gene description and chromosome location.

3.4. Gene ontology and pathway analysis

One of the important steps in a standard transcriptomics study is the characterization of the molecular functions or pathways in which DEGs are involved by comparing a list of DEGs against the rest of the genome for over-represented functions, and gene set enrichment analysis, which is based on ranking the transcriptome according to the measurement of differential expression (Conesa et al., 2016). In this sense, the over-representation analysis using ConsensusPathDB of the selected 43 DEGs geneset provided a list of gene ontology (GO) terms in which several biological processes related to respiratory and electron transport chain, oxidative phosphorylation, cellular respiration, generation of precursor metabolites and energy, mitochondrial respiratory chain complex I biogenesis and assembly, etc. were most over-represented. Molecular functions linked to oxidoreductase activity, NADH dehydrogenase and NADH dehydrogenase (quinone) activity were statistically more significative in the DEGs set, while cellular components such as mitochondrial membrane, mitochondrial respiratory chain, mitochondrial envelope, NADH dehydrogenase and oxidoreductase complexes, mitochondrial protein complex and respiratory chain were significantly represented in BEA treated Jurkat cells compared to control samples.

Pathway analysis using PathVisio showed a total of 7688 data points (N) and an increased number of data points meeting criterion (R) with increasing doses, i.e. 26, 1096 and 2398 for 1.5, 3 and 5 µM, respectively. When all concentrations data where integrated 25 data points meeting criterion (R) were overlapped. Three pathways were statistically significant in the three studied doses (z-score > 1.96; adj *p*-value < 0.05); oxidative phosphorylation, electron transport chain and nucleotide metabolism. Moreover, the number of genes involved in the pathways, as well as, the percentage of positive/measured genes showed a dose-dependent relationship. The analysis revealed 6, 23 and 50 DEGs included in the oxydative phosphorylation pathway for 1.5, 3 and 5 µM, respectively, with the highest z-score (12.99) among all the pathways. Furthermore, electron transport chain pathway (z-score: 11.61) included 7, 36 and 82 DEGs, while nucleotide metabolism pathway (z-score: 3.79) showed 1, 7 and 16 DEGs for 1.5, 3 and 5 µM, respectively (Fig. 3). Other statistically significant pathways were found overlapped in the two highest BEA concentrations (3 and 5 µM), such as DNA damage response, G1 to S cell cycle control, and integrated cancer pathway.

Fig. 4 shows the genes invoved in the electron transport chain pathway for Homo sapiens, indicating in red and blue the down-regulated and up-regulated genes, respectively, for the three BEA concentrations (1.5, 3 and 5 µM).

3.5. Functional profiling of DEGs

The whole list of 5719 DEGs included several genes belonging to ATPase H+ transporting subunits, cytochrome c oxidase subunits, NADH: ubiquinone oxidoreductase subunits, ubiquinol-cytochrome c reductases, ribosomal proteins, and mitochondrial ribosomal proteins, among others. All DEGs were individually characterized and studied to find relevant genesets related to some specific biological routs and pathways. In this way, functional related gene groups mainly belonging to respiratory chain, apoptosis, necrosis process, and caspases cascade activation were deeply studied.

3.5.1. Respiratory chain

Respiration is the core of mitochondrial metabolism for free energy release and ATP production, and depends on the function of the electron transport chain, composed of five respiratory complexes (Qi et al., 2017). During respiration, electrons from NADPH and FADH2 are transferred to O_2 generating ATP and oxidized NADP1 and FAD1. Depending on the substrate, electrons are transported from complex I

Table 2
43 DEGs (for all BEA concentrations): HGNC Symbol, gene description, and chromosome location.

HGNC Symbol	Gene Desription	Location
MT-CYB	mitochondrially encoded cytochrome b	Chr. MT
MT-ND3	mitochondrially encoded NADH:ubiquinone oxidoreductase core subunit 3	Chr. MT
MT-ATP6	mitochondrially encoded ATP synthase 6	Chr. MT
MTATP6P1	mitochondrially encoded ATP synthase 6 pseudogene 1	Chr. 1
MT-CO3	mitochondrially encoded cytochrome c oxidase III	Chr. MT
MT-ND5	mitochondrially encoded NADH:ubiquinone oxidoreductase core subunit 5	Chr. MT
MT-ATP8	mitochondrially encoded ATP synthase 8	Chr. MT
MT-ND4	mitochondrially encoded NADH:ubiquinone oxidoreductase core subunit 4	Chr. MT
MT-ND2	mitochondrially encoded NADH:ubiquinone oxidoreductase core subunit 2	Chr. MT
MT-ND4L	mitochondrially encoded NADH:ubiquinone oxidoreductase core subunit 4L	Chr. MT
MATN4	matrilin 4	Chr. 20
SRM	spermidine synthase	Chr. 1
MRPL12	mitochondrial ribosomal protein L12	Chr. 17
APRT	adenine phosphoribosyltransferase	Chr. 16
PPIB	peptidylprolyl isomerase B	Chr. 15
PDIA4	protein disulfide isomerase family A member 4	Chr. 7
PPAN	peter pan homolog (Drosophila)	Chr. 19
CCDC86	coiled-coil domain containing 86	Chr. 11
YBX3	Y-box binding protein 3	Chr. 12
EIF5A	eukaryotic translation initiation factor 5A	Chr. 17
CHCHD2	coiled-coil-helix-coiled-coil-helix domain containing 2	Chr. 7
CCDC124	coiled-coil domain containing 124	Chr. 19
MRPL4	mitochondrial ribosomal protein L4	Chr. 19
CDK2AP2	cyclin dependent kinase 2 associated protein 2	Chr. 11
PFN1	profilin 1	Chr. 17
PPP1R14B	protein phosphatase 1 regulatory inhibitor subunit 14 B	Chr. 11
CPNE1	copine 1	Chr. 20
PLK1	polo like kinase 1	Chr. 16
COTL1	coactosin like F-actin binding protein 1	Chr. 16
SEC13	SEC13 homolog, nuclear pore and COPII coat complex component	Chr. 3
YBX1	Y-box binding protein 1	Chr. 1
ARHGDIA	Rho GDP dissociation inhibitor alpha	Chr. 17
ACTB	actin beta	Chr. 7
LAT	linker for activation of T-cells	Chr. 16
ALDOA	aldolase, fructose-bisphosphate A	Chr. 16
CSK	c-src tyrosine kinase	Chr. 15
OGT	O-linked N-acetylglucosamine (GlcNAc) transferase	Chr. X
EDEM1	ER degradation enhancing alpha-mannosidase like protein 1	Chr. 3
ARPP21	cAMP regulated phosphoprotein 21	Chr. 3
INSIG1	insulin induced gene 1	Chr. 7
MGEA5	meningioma expressed antigen 5 (hyaluronidase)	Chr. 10
TXNIP	thioredoxin interacting protein	Chr. 1
MT-RNR2	mitochondrially encoded 16S RNA	Chr. MT

(NADH dehydrogenase [ubiquinone]) and complex II *(succinate dehydrogenase)* through ubiquinone and complex III *(ubiquinol-cytochrome c reductase)* to cytochrome-c and to complex IV *(cytochrome-c oxidase)*, which produces water, while ATP is generated by complex V *(ATP synthase)* (Dudkina et al., 2006).

In the present study several genes related to respiratory chain were significantly altered. From the 96 genes involved in the respiratory chain (HGNC database), 77 genes were differentially expressed at least at one dose (all down-regulated), indicating that BEA induced perturbation of 80% of the respiratory chain genes. Although the 5 complexes were affected, complex I, complex III, and complex V showed the highest number of perturbed genes (84–90%). Among these 77 genes, 9 were differentially expressed for all three BEA concentrations, mainly belonging to complex I (5 genes), followed by complex V (2 genes), and complexes III and IV (1 gene each). As shown in Fig. 5, all 9 genes were down-regulated in a clear dose-dependent manner.

Similar gene expression results were recently observed by microarray technique after 4 h expossure of the emerging mycotoxin EN B (1, 10 and 20 μM) on rat primary hepatocytes. The number of down-regulated genes was five times higher than up-regulated ones, with over-represented genes associated with apoptotic processes, apoptotic mitochondrial changes, and cell signal transduction. Moreover, it was revealed the alteration of energy metabolism due to effects on mitochondrial organization and function, and the assembly of complex I of the electron transport chain (Jonsson et al., 2016).

3.5.2. Necrosis, apoptosis and programmed cell death

Cell death generally proceeds through two molecular mechanisms: necrosis and apoptosis. Apoptosis is highly regulated cell death program triggered through the extrinsic (or death receptors) pathway or the intrinsic (or mitochondrial) pathway (Boussabbeh et al., 2015). It is considered an important physiological process involved in cell deletion during organogenesis and in the control of cell proliferation and differentiation in adult tissues, which characterized by distinct biochemical features. Apoptosis can be triggered by numerous mediators including receptor-mediated signals, withdrawal of growth factors, and environmental agents (Elmore, 2007). In the present study 21 genes (14 down-regulated and 7 up-regulated) related to apoptosis and programmed cell death were differentially expressed at least at one dose (5 μM and/or 3 μM). On the other hand, 4 necrosis related genes were perturbed (3 down-regulated and 1 up-regulated) but only in treated Jurkar cells with the highest BEA concentration (5 μM), while low (1.5 μM) and medium (3 μM) BEA doses did not show significant alteration in the expression of the necrosis involved genes. Fig. 6 shows the differentially expressed genes related to apoptosis and programmed cell death (3 and 5 μM), and genes linked to necrosis process (5 μM).

The cytotoxicity of BEA has been previously described based on apoptosis induction via the mitochondrial pathway for several human cancer cell lines; such as non small cell lung cancer [NSCLC] A549 (Lu et al., 2016; Lin et al., 2005), acute lymphoblastic leukemia [CCRF-

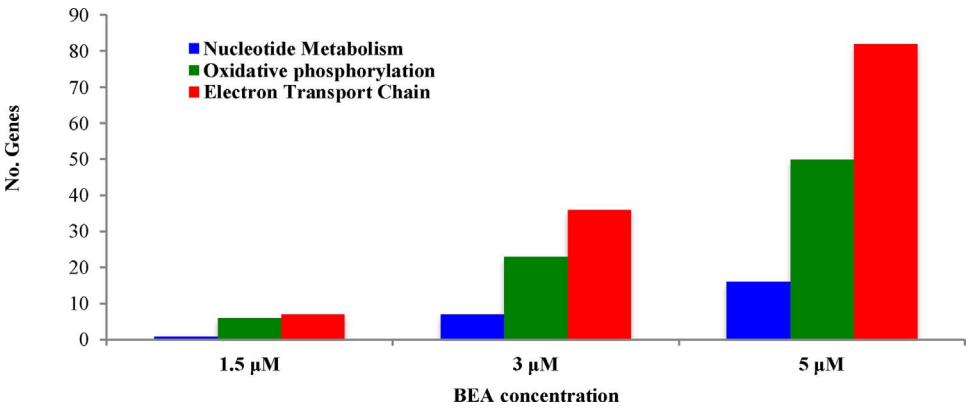

Fig. 3. Number of DEGs involved in the oxydative phosphorylation, electron transport chain, and nucleotide metabolism pathways for the three BEA concentrations (1.5, 3 and 5 μM).

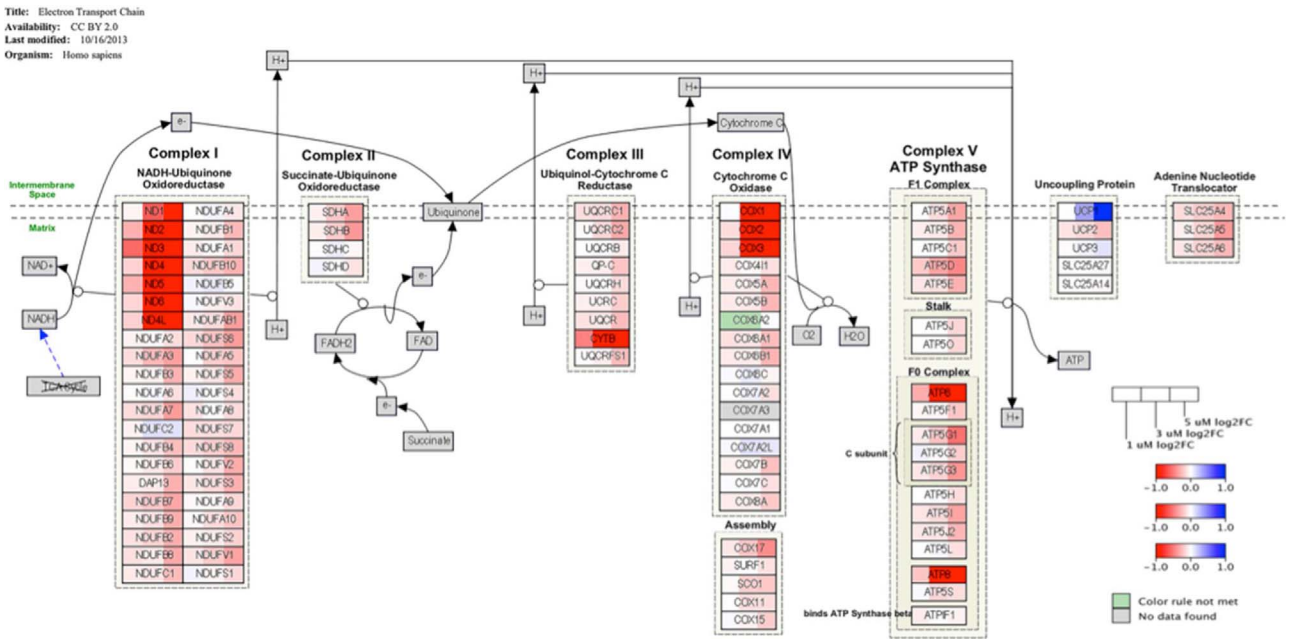

Fig. 4. Electron transport chain pathway (*Homo sapiens*) obtained with the DEGs by PathVisio analysis. Highlighted in red the down-regulated and in blue the up-regulated genes for the three BEA concentrations (1.5, 3 and 5 μM). (For interpretation of the references to colour in this figure legend, the reader is referred to the web version of this article.)

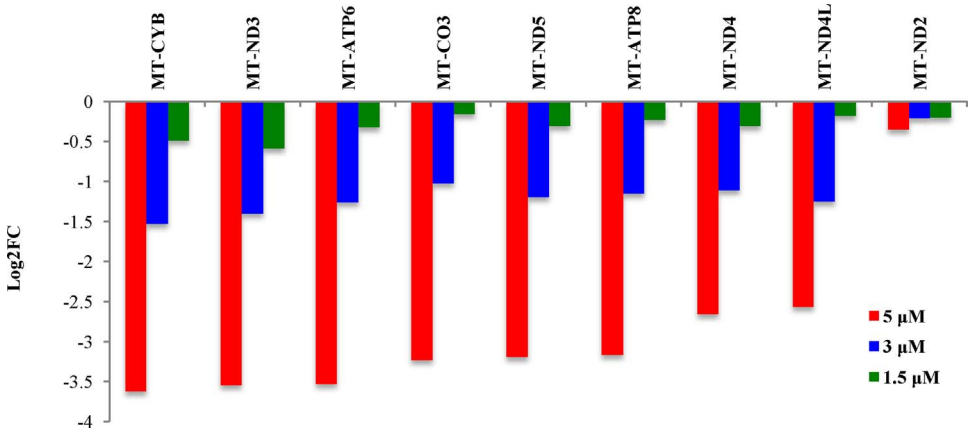

Fig. 5. Respiratory chain genes altered in the three BEA concentrations; 1.5, 3 and 5 μM.

CEM] (Jow et al., 2004), cervix carcinoma [KB, KBv200 and KB-3-1] (Tao et al., 2015; Dornetshuber et al., 2009), and colon adenocarcinoma [Caco-2] (Prosperini et al., 2013). Moreover, BEA induced apoptosis in activated T cells (Wu et al., 2013), Chinese hamster ovary [CHO-K1] (Mallebrera et al., 2016), rat liver hepatoma [H4IIE] (Watjen et al., 2014), porcine kidney PK15 (Klaric et al., 2008), turkey peripheral blood lymphocytes (Dombrink-Kurtzman, 2003), and rodent cholangiocytes (Que et al., 1997). However, the molecular mechanism

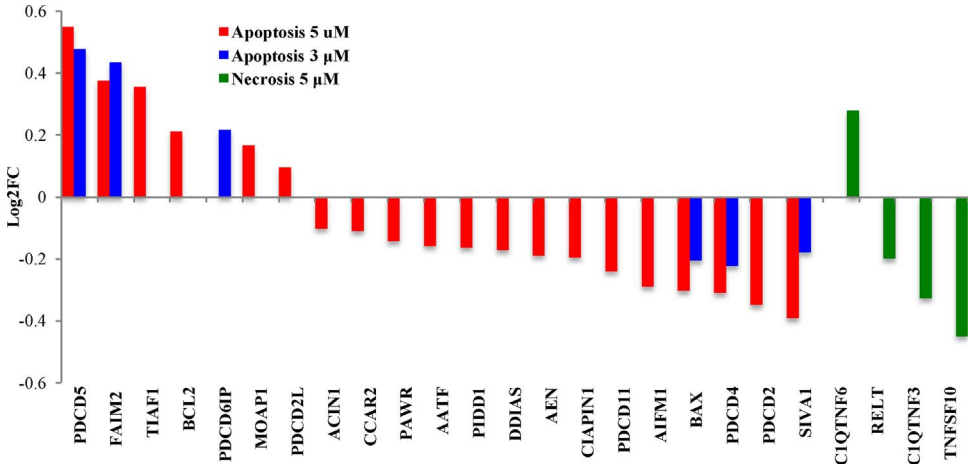

Fig. 6. Apoptosis and necrosis related genes altered in Jurkat cells treated with 3 and/or 5 μM BEA (apoptosis), and with 5 μM BEA (necrosis), respectively.

underlying the BEA-induced apoptotic process is not yet clearly understood (Lin et al., 2005). The available literature demonstrated that the induction of apoptosis by BEA involves multiple cellular/molecular pathways and the molecular mechanisms are still controversially discussed. BEA ionophoric action could be responsible for the alteration of the lipid membrane structures and production of ROS, which decrease intracellular GSH content, contributing to apoptosis and necrosis (Klaric et al., 2008). Some studies showed that BEA induced apoptosis by decreasing the mitochondrial membrane potential, which leads to the release of cytochrome c into cytosol and caspase-3 activation. Loss of mitochondrial membrane potential may be an early event in the apoptotic process and required for BEA-induced cytochrome c release into cytosol, that later triggered the cleavage and activation of mitochondrial downstream caspases (Lin et al., 2005). However, it may not be an early requirement for apoptosis and may be a consequence of the apoptotic-signaling pathway (Ly et al., 2003). It was also suggested that intracellular Ca^{2+} plays an important role as a mediator in cell death signalling induced by BEA, since it increases cytosolic Ca^{2+} concentration in a dose-dependent manner leading to irreversible cell damage if it is not immediately compensated (Chen et al., 2006). Moreover, the rise in Ca^{2+} is a point of convergence among many downstream mechanisms, i.e., decreases the mitochondial membrane potential, releases of cytochrome c, increases caspase activation and apoptosis (Mallebrera et al., 2016). Other results showed that mitochondrial integrity and apoptosis were mainly regulated by the expression of Bcl-2 family proteins of cell death regulatory molecules (Lee et al., 2008).

An increase in early apoptotic cells was observed in Caco-2 and CHO-K1 cells with inhibition of cell proliferation arresting cells in G0/G1 (Prosperini et al., 2013; Mallebrera et al., 2016). In human NSCLC A549 cells BEA-induced apoptosis in concentration- and time-dependent manner by mitochondrial transmembrane depolarization and significant reduction of mitochondrial membrane potential, increase in the release of mitochondrial cytochrome c, and activation of caspase 3 (Lin et al., 2005). Significant increase of apoptosis was later reported in the same cell line by the activation of MEK1/2 (mitogen-activated protein kinase)-ERK42/44 (extracellular signal-regulated kinases)-90RSK (ribosomal s6 kinase) signaling pathway, with the up-regulation of the pro-apoptotic proteins Bax, Bak, Bad, and down-regulation of anti-apoptotic protein Bcl-2 (Lin et al., 2005). BEA inhibited activated T cells via PI3 K/Akt inhibition, thereby suppressing cell activation/proliferation, reducing cytokines production and resulting in cell apoptosis, by collapse of mitochondrial membrane potential, release of cytochrome c to the cytosol, down-regulation of Bcl-2, phosphorylation of Bad, activation of caspase-12, 9, 3 and PARP cleavage (Wu et al., 2013). Apoptosis by mitochondrial pathway, including decrease of ROS generation, loss of mitochondrial membrane potential, release of cytochrome c, activation of Caspase-9 and −3, and cleavage of PARP was also described in KB and KBv200 cells, without signs of Bcl-2 or Bax alteration (Tao et al., 2015). In human promyelocytic leukaemia cells (HL60) and human cervix carcinoma cells (KB-3-1) cells generation of ROS was not involved in BEA-induced apoptosis (Dornetshuber et al., 2009).

On the other hand, cell death by necrosis as the ultimate endpoint of lethal cell injury has been also reported, nevertheless apoptosis remains as the main cell death process induced by BEA exposure. Increased necrotic CHO-K1 cells was observed after 48 h of exposure, although BEA 24 h exposure produced apoptosis but not necrosis (Mallebrera et al., 2016). Necrosis was evidenced in C6 glioma BEA exposed cells, but apoptosis prevails in H4IIE hepatoma cells with significant increase in caspase 3/7 activity and nuclear fragmentation, as a molecular mechanism of cell death (Watjen et al., 2014). Apoptosis and necrosis were observed in porcine kidney PK15 cells depending on the concentration used and time of exposure, with an increase in caspase-3 activity after 48 h of exposure leading to apoptosis (Klaric et al., 2008).

3.5.3. Caspase cascade

Caspases have been shown to be activated during apoptosis in many cell systems and play critical roles in both the initiation and execution of apoptosis (Jow et al., 2004). Caspases are expressed as inactive proenzymes in living cells and become activated when cells receive an apoptosis- inducing signal. Once activated, they cleave a number of key substrates, resulting in their activation or inactivation. Activation of caspases leads to the morphological and biochemical features of apoptosis. Two caspase activating cascades that regulate apoptosis have been described: one is initiated from the cell surface death receptor and the other is triggered by changes in mitochondria integrity (Yuan et al., 2003). A family of at least 13 related cysteine proteases has been identified in mammals, existing in the cell as inactive precursors that undergo proteolytic processing and activation. Once activated, initiator caspases can proteolyse additional effector caspases, generating a proteolytic cascade that cleaves key structural components as well as proteins critical for cell survival in a highly sequence-specific fashion, ultimately resulting in the systemic and controlled destruction of the cell (Donovan and Cotter, 2004).

In the present study, 12 genes involved in caspase cascade activation were differentially expressed (10 up-regulated and 2 down-regulated) at least at one BEA dose (3 and/or 5 µM), pointing to mainly affect initiator caspases 8, 9 and 10 (Fig. 7).

Activation of caspase 3, which can occur as a consequence of caspase 9 activation, is a central mechanism of apoptosis in the death receptor pathway, leading to intracellular events in the apoptosis cascade, and essential for DNA fragmentation (Jow et al., 2004; Lin et al., 2005). Since the apoptosome cascade or intrinsic pathway involves activation of procaspase 9 by cytochrome c released from the mitochondria (Lee et al., 2008), gene expression alteration of initiator caspases shown in

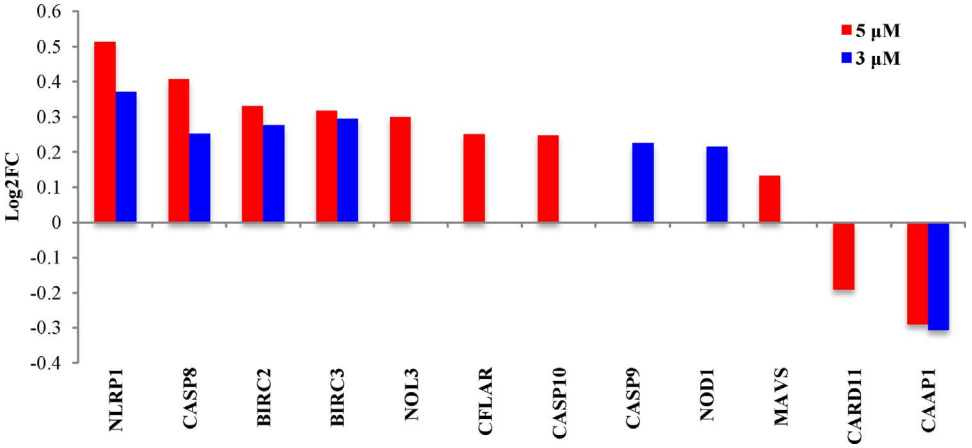

Fig. 7. Caspases cascade related genes altered in Jurkat cells treated with 3 and 5 µM BEA concentrations for 24 h.

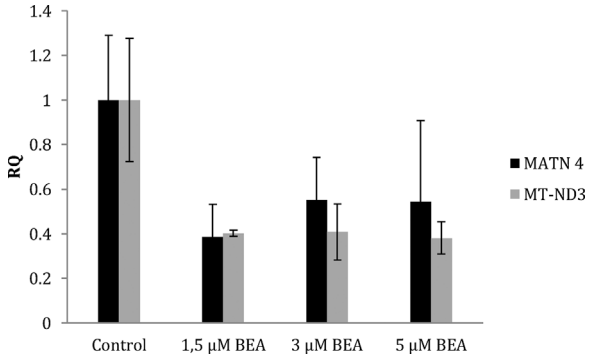

Fig. 8. Bar plot showing Jurkat cells relative expression of selected genes when compared to control (RQ = 1) after 24h-exposure to different concentrations of BEA by qPCR. RQ, relative quantification.

the present study may indicate an apoptosis early step, which may lead to the activation of the executioner procaspases (caspase 3, 6 and 7) that cleave PARP and other apoptotic protein substrates. Recent results obtained in our laboratory showed that BEA induced apoptosis in Jurkat cells after 24 and 48 h exposure in a concentration and time dependent manner. Moreover, caspase-3 activation was already observed after 24 h of BEA exposure and reached 60% of activated cells after 48 h (data not shown).

Summarizing, the perturbed genes involved in apoptosis and programmed cell death identified in the present study showed overall trend towards apoptosis after BEA exposure in Jurkat cells. In this way PDCD5, which encodes a protein over-expressed during apoptosis, and MOAP1, which mediates caspase-dependent apoptosis, were up-regulated. On the other hand, the up-regulation of caspases genes CASP8, CASP9, CASP10 and NLRP1 gene, known to be key mediator of programmed cell death whose over-expression induce apoptosis by strongly interaction with caspase 2 and weakly with caspase 9, supports the apoptosis induction by BEA. Moreover, the down-regulation of CAAP1, a caspase activity and apoptosis inhibitor that encodes and anti-apoptotic protein modulator of caspase-10 dependent mitochondrial and caspase-3/9 feedback amplification loop is in agreement with the apoptosis path. Nevertheless, some specific genes perturbation, such as the up-regulation of NOL3 −anti-apoptotic gene- could not be explained. With regard to the bcl-2 family genes, the present study showed down-regulation of Bax and up-regulation of Bcl-2, contrary to other studies where the up-regulation of the pro-apoptotic protein Bax and the down-regulation of anti-apoptotic protein Bcl-2 were reported, among with caspases genes up-regulation (Lin et al., 2005; Wu et al., 2013). Either Bcl-2 is up-regulated and Bax down-regulated to attenuate BEA induced apoptosis or Bcl-2 may act as a downstream death substrate of caspases, i.e. Bcl-2 is cleaved by caspase 3, thereby not only inactivating its anti-apoptotic function but also enhancing cell death (Cheng et al., 1997). Eitherway, the results shown in the present work still agree with the other studies with regard to the caspases activation as main possible path for the apoptosis event.

3.6. Confirmation of NGS results by PCR

The sequencing-based results were validated using qPCR. The expression of MT-ND3, a mitochondrial DNA gene, and MATN4, a nuclear DNA gene, was measured in Jurkat cells after exposure to BEA in the same conditions than in the NGS assay. The results confirm the down-regulation of both genes compared to the control (Fig. 8).

House-keeping gene 18S rRNA was used as endogenous gene control (Fig. 8). S18 has not been differently expressed at any concentration exposed and it has already been valited as a good house-keeping gene (Banda et al., 2008).

4. Conclusion

This is – to our knowledge – the first transcriptomic study based on RNA-seq addressing BEA cytotoxicity in human Jurkat lymphoblastic T cells. The transcriptomic analysis revealed that BEA altered gene expression profile in the human genome in a dose-dependent manner. RNA-seq showed a large number of differentially expressed genes mainly related to respitatory chain, apoptosis, and caspase cascade activation. Biological processes related to respiratory and electron transport chain, oxidative phosphorylation, and cellular respiration were most over-represented. Molecular functions linked to oxidoreductase activity, NADH dehydrogenase and NADH dehydrogenase (quinone) activity were statistically more significative in the DEGs set, while cellular components such as mitochondrial membrane, mitochondrial respiratory chain, mitochondrial envelope, NADH dehydrogenase and oxidoreductase complexes, mitochondrial protein complex, and respiratory chain were significantly represented in BEA treated Jurkat cells compared to control samples. Finally, oxidative phosphorylation, electron transport chain, and nucleotide metabolism pathways were dose-dependent significantly altered in the three studied concentrations (z-score > 1.96; adj p-value < 0.05). These results assist in understanding the mechanisms of BEA induced cytotoxicity and strongly suggest the implication of mitochondrial damage pointing to apoptosis through the caspase cascade activation in human lymphoblastic T cells.

Conflict of interest

None.

Acknowledgement

This work was supported by the Spanish Ministry of Economy and Competitiveness (AGL2016-77610-R and BES-2014-068039).

References

Andrews, S., 2010. FastQC: a Quality Control Tool for High Throughput Sequence Data. Available online at: http://www.bioinformatics.babraham.ac.uk/projects/fastqc.

Banda, M., Bommineni, A., Thomas, R.A., Luckinbill, L.S., Tucker, J.D., 2008. Evaluation and validation of housekeeping genes in response to ionizing radiation and chemical exposure for normalizing RNA expression in real-time PCR. Mutat. Res. Genet. Toxicol. Environ. Mutag. 649, 126–134.

Boussabbeh, M., Salem, I.B., Prola, A., Guilbert, A., Bacha, H., Abid-Essefi, S., Lemaire, C., 2015. Patulin induces apoptosis through ROS-Mediated endoplasmic reticulum stress pathway. Toxicol. Sci. 144, 328–337.

Bustin, S.A., Benes, V., Garson, J.A., Hellemans, J., Huggett, J., Kubista, M., Mueller, R., Nolan, T., Pfaffl, M.W., Shipley, G.L., Vandesompele, J., Wittwer, C.T., 2009. The MIQE guidelines: minimum information for publication of quantitative real-time PCR experiments. Clin. Chem. 55, 611–622.

Caiment, F., Gaj, S., Claessen, S., Kleinjans, J., 2015. High-throughput data integration of RNA–miRNA–circRNA reveals novel insights into mechanisms of benzo [a] pyrene-induced carcinogenicity. Nucleic Acids Res. 43, 2525–2534.

Celik, M., Aksoy, H., Yılmaz, S., 2010. Ecotoxicology and Environmental Safety Evaluation of beauvericin genotoxicity with the chromosomal aberrations, sister-chromatid exchanges and micronucleus assays. Ecotoxicol. Environ. Saf. 73, 1553–1557.

Chen, B.-F., Tsai, M.-C., Jow, G.-M., 2006. Induction of calcium influx from extracellular fluid by beauvericin in human leukemia cells. Biochem. Biophys. Res. Commun. 340, 134–139.

Cheng, E.H.-Y., Kirsch, D.G., Clem, R.J., Ravi, R., Kastan, M.B., Bedi, A., Ueno, K., Hardwick, J.M., 1997. Conversion of bcl-2 to a bax-like death effector by caspases. Science 278, 1966–1968.

Conesa, A., Madrigal, P., Tarazona, S., Gomez-Cabrero, D., Cervera, A., McPherson, A., Szcześniak, M.W., Gaffney, D.J., Elo Zhang, L.L.X., Mortazavi, A., 2016. A survey of best practices for RNA-seq data analysis. Genome Biol. 17 :13, 1–19. http://dx.doi.org/10.1186/s13059-016-0881-8.

Dellafiora, L., Dall'Asta, C.D., 2017. Forthcoming challenges in mycotoxins toxicology research for safer food – a need for multi-omics approach. Toxins 9, 18.

Dombrink-Kurtzman, M.A., 2003. Fumonisin and beauvericin induce apoptosis in turkey peripheral blood lymphocytes. Mycopathologia 156, 357–364.

Donovan, M., Cotter, T.G., 2004. Control of mitochondrial integrity by Bcl-2 family members and caspase-independent cell death. Biochim. Biophys. Acta 1644, 133–147.

Dornetshuber, R., Heffeter, P., Lemmens-Gruber, R., Elbling, L., Marko, D., Micksche, M., Berger, W., 2009. Oxidative stress and DNA interactions are not involved in Enniatin- and Beauvericin-mediated apoptosis induction. Mol. Nutr. Food Res. 53, 1112–1122.
Dudkina, N.V., Heinemeyer, J., Sunderhaus, S., Boekema, E.J., Braun, H.P., 2006. Respiratory chain supercomplexes in the plant mitochondrial membrane. Trends Plant Sci. 11, 232–240.
Elmore, S., 2007. Apoptosis: a review of programmed cell death. Toxicol. Pathol. 35, 495–516.
Escrivá, L., Font, G., Manyes, L., 2015. In vivo toxicity studies of Fusarium mycotoxins in the last decade: a review. Food Chem. Toxicol. 78, 185–206.
Fang, Z., Martin, J., Wang, Z., 2012. Statistical methods for identifying differentially expressed genes in RNA-seq experiments. Cell Biosci. 2, 26.
Jonsson, M., Jestoi, M., Anthoni, M., Welling, A., Loivamaa, I., Hallikainen, V., Kankainen, M., Lysøe, E., Koivisto, P., Peltonen, K., 2016. Toxicology in Vitro Fusarium mycotoxin enniatin B: cytotoxic effects and changes in gene expression profile. Toxicol. In Vitro 34, 309–320.
Jow, G.-M., Chou, C.-J., Chen, B.-F., Tsai, J.-H., 2004. Beauvericin induces cytotoxic effects in human acute lymphoblastic leukemia cells through cytochrome C release, caspase 3 activation: the causative role of calcium. Cancer Lett. 216, 165–173.
Katika, M.R., Hendriksen, P.J.M., Shao, J., van Loveren, H., Peijnenburg, A., 2012. Transcriptome analysis of the human T lymphocyte cell line Jurkat and human peripheral blood mononuclear cells exposed to deoxynivalenol (DON): New mechanistic insights. Toxicol. Appl. Pharmacol. 264, 51–64.
Klaric, M.S., Rumora, R., Ljubanovic, D., Pepeljnjak, S., 2008. Cytotoxicity and apoptosis induced by fumonisin B1, beauvericin and ochratoxin A in porcine kidney PK15 cells: effects of individual and combined treatment. Arch. Toxicol. 82, 247–255.
Lee, H.-J., Lee, H.-J., Lee, E.-O., Ko, S.-G., Bae, H.-S., Kim, C.-H., Ahn, K.-S., Lu, J., Kim, S.-H., 2008. Mitochondria-cytochrome C-caspase-9 cascade mediates isorhamnetin-induced apoptosis. Cancer Lett. 270, 342–353.
Li, Z., Long, Y., Zhong, L., Song, G., Zhang, X., Yuan, L., Cui, Z., Dai, H., 2016. RNA sequencing provides insights into the toxicogenomic response of ZF4 cells to methyl methanesulfonate. J. Appl. Toxicol. 36, 94–104.
Lin, H.-I., Lee, Y.-J., Chen, B.-F., Tsai, M.-C., Lu, J.-L., Chou, C.-J., Jow, G.-M., 2005. Involvement of Bcl-2 family, cytochrome c and caspase 3 in induction of apoptosis by beauvericin in human non-small cell lung cancer cells. Cancer Lett. 230, 248–259.
Lu, C.-H., Lin, H.-I., Chen, B.-F., Jow, G.-M., 2016. Beauvericin-induced cell apoptosis through the mitogen-activated protein kinase pathway in human nonsmall cell lung cancer A549 cells. J. Toxicol. Sci. 41, 429–437.
Mallebrera, B., Font, G., Ruiz, M.J., 2014. Disturbance of antioxidant capacity produced by beauvericin in CHO-K1 cells. Toxicol. Lett. 226, 337–342.
Mallebrera, B., Juan-Garcia, A., Font, G., Ruiz, M.J., 2016. Mechanisms of beauvericin toxicity and antioxidant cellular defense. Toxicol. Lett. 246, 28–34.
Manyes, L., Escrivá, L., Serrano, A.B., Rodríguez-Carrasco, Y., Tolosa, J., Meca, G., Font, G., 2014. A preliminary repeated dose 28-day oral study in Wistar rats with enniatin A contaminated feed. Toxicol. Mech. Methods 24, 179–190.
Prosperini, A., Juan-García, A., Font, G., Ruiz, M.J., 2013. Beauvericin-induced cytotoxicity via ROS production and mitochondrial damage in Caco-2 cells. Toxicol. Lett. 222, 204–211.
Qi, W., Tian, Z., Lu, L., Chen, X., Chen, X., Zhang, W., Song, R., 2017. Editing of mitochondrial transcripts nad3 and cox2 by dek10 is essential for mitochondrial function and maize plant development. Genetics 205, 1489–1501.
Que, F.G., Gores, G.J., LaRusso, N.F., 1997. Development and initial application of an in vitro model of apoptosis in rodent cholangiocytes. Am. Physiol. Soc. 272, 106–115.
Ruiz, M.J., Franzova, P., Font, G., 2011. Toxicological interactions between the mycotoxins beauvericin: deoxynivalenol and T-2 toxin in CHO-K1 cells in vitro. Toxicon 58, 315–326.
Schoevers, E.J., Santos, R.R., Fink-Gremmels, J., Roelen, B.A.J., 2016. Toxicity of beauvericin on porcine oocyte maturation and preimplantation embryo development. Reprod. Toxicol. 65, 159–169.
Shao, J., Berger, L.F., Hendriksen, P.J.M., Peijnenburg, A.A.C.M., van Loveren, H., Volger, O.L., 2014. Transcriptome-based functional classifiers for direct immunotoxicity. Arch. Toxicol. 67, 3–689.
Smith, M.-C., Madec, S., Coton, E., Hymery, N., 2016. Natural Co-Occurrence of mycotoxins in foods and feeds and their in vitro combined toxicological effects. Toxins 8, 94.
Tao, Y.-W., Lin, Y.-X., She, Z.-G., Lin, M.-T., Chen, P.-X., Zhang, J.-Y., 2015. Anticancer activity and mechanism investigation of beauvericin isolated from secondary metabolites of the mangrove endophytic fungi. Anticancer Agents Med. Chem. 15, 258–266.
Tonshin, A.A., Teplova, V.V., Andersson, M.A., Salkinoja-Salonen, M.S., 2010. The Fusarium mycotoxins enniatins and beauvericin cause mitochondrial dysfunction by affecting the mitochondrial volume regulation, oxidative phosphorylation and ion homeostasis. Toxicology 276, 49–57.
Wang, Q., Xu, L., 2012. Beauvericin, a bioactive compound produced by fungi: a short review. Molecules 236, 7–2377.
Watjen, W., Debbab, A., Hohlfeld, A., Chovolou, Y., Proksch, P., 2014. The mycotoxin beauvericin induces apoptotic cell death in H4IIE hepatoma cells accompanied by an inhibition of NF-kB-activity and modulation of MAP-kinases. Toxicol. Lett. 231, 9–16.
Wen, J., Mu, P., Deng, Y.1, 2016. Mycotoxins: cytotoxicity and biotransformation in animal cells. Toxicol. Res. 5, 377–387.
Wilson, V.S., Keshava, N., Hester, S., Segal, D., Chiu, W., Thompson, C.M., Euling, S.Y., 2013. Utilizing toxicogenomic data to understand chemical mechanism of action in risk assessment. Toxicol. Appl. Pharmacol. 271, 299–308.
Wu, X.-F., Xu, R., Ouyang, Z.-J., Qian, C., Shen, Y., Wu, X.-D., Gu, Y.-J., Xu, Q., 2013. Sun Y.(2013) beauvericin ameliorates experimental colitis by inhibiting activated t cells via downregulation of the PI3 K/Akt signaling pathway. PLoS One e83013.
Yuan, J., Murrell, G.A.C., Trickett, A., Wang, M.-X., 2003. Involvement of cytochrome c release and caspase-3 activation in the oxidative stress-induced apoptosis in human tendon fibroblasts. Biochim. Biophys. Acta 1641, 35–41.